SINGLE-FEED CIRCULARLY POLARIZED ANNULAR SLOT ANTENNA FOR DUAL-BROADBAND OPERATION

Yuan-Ming Cai[*], Shu-Feng Zheng, Ying-Zeng Yin, Jiao-Jiao Xie, and Ke Li

National Laboratory of Science and Technology on Antennas and Microwaves, Xidian University, Xi'an, Shaanxi 710071, P. R. China

Abstract—A novel dual-broadband circularly polarized folded slot antenna with single-feed is presented. The proposed antenna consists of two folded annular slots. By adjusting the asymmetric widths of the two slots, circularly polarized radiation can be achieved in two different bands. By optimizing the parameters of the proposed antenna, two wide impedance bandwidths of 35.0% (1.91–2.72 GHz) and 46.5% (4.36–7.00 GHz) can be obtained, and two axial ratio bandwidths are 2.36–2.56 GHz and 5.68–6.04 GHz, respectively. The antenna with simple structure is fabricated and measured. Good agreement between the simulated and measured results is also achieved.

1. INTRODUCTION

Circular polarization and dual-band operation are usually desired characteristics for antennas in modern wireless systems [1–10]. Meanwhile, printed slot antennas are commonly used in communication system due to their advantages such as low profile, wide bandwidth, low cost and ease of fabrication. Several dual-band slot antenna designs with good characteristics were proposed in [1–5]. However, these antennas were only designed for linear polarized. Several designs have been reported to produce circular polarization [6–10], but all these design only realize one CP radiation band.

A dual-frequency CP microstrip antenna was presented in [11]. However, the antenna has double dielectric layers structure, which increases the complexity and difficulty in manufactory and assemble process. There are several designs using single-layered substrate to

realize circular polarization. In [12], dual-band circularly polarized annular slot antenna is obtained by employing two square slots, a bended microstrip line and a cavity back. Dual-band CP radiation can also be achieved by using a spiral slot [13], or a CPW-fed annular slot with two perturbation strips [14]. In [15], a square microstrip patch antenna embedded with four slots and a crossed slot can generate dual-band CP radiation. But all these designs in [13–15] have a limited range of the frequency ratio.

In this paper, a novel dual-broadband circularly polarized antenna using two special slots and single microstrip-coupled feed is introduced and investigated. By optimizing the key geometrical parameters of the antenna, two wide impedance bandwidths of 35.0% (1.91–2.72 GHz) and 46.5% (4.36–7.00 GHz) are obtained, as well as two axial ratio bandwidths are 2.36–2.56 GHz and 5.68–6.04 GHz, respectively. Good agreement between the simulated and measured results is also achieved, which implies that the proposed antenna is a good candidate for dual-broadband circularly polarized wireless systems.

2. ANTENNA DESIGN

The configuration of the proposed antenna is showed in Figure 1. The antenna is printed on a square PTFE dielectric substrate with a relative permittivity of $\varepsilon_r = 2.65$, a side length of the substrate G is 50 mm and a thickness h is 1 mm. Two annular slots are etched on the bottom side of the substrate. They are excited by a modified microstrip transmission line printed on top side of the substrate.

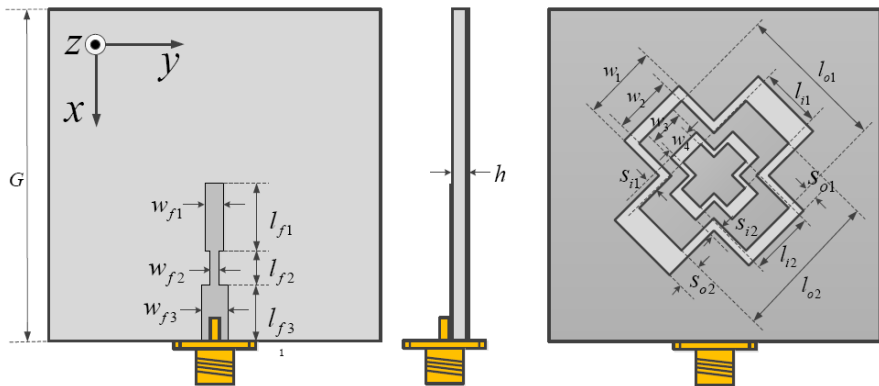For conventional annular slot, the wavelength of the fundamental

Figure 1. Configuration of the proposed antenna.

resonant mode almost equals to the mean circumference of the slot. By adjusting the width of the slot (S_{o1} and S_{o2}, or S_{i1} and S_{i2}), the symmetric fold annular slot will be also perturbed at the same time. And then the fundamental resonant mode will be split into two orthogonal degenerate modes. With the appropriate perturbation, the two orthogonal degenerate modes of the annular slot can be excited with 90° phase difference and CP radiation will be realized.

The design evolution of the proposed antenna and the corresponding simulated return loss curves are shown in Figure 3. In this design, the geometrical parameters of the antennas are studied with the aid of ANSYS High Frequency Structure Simulator (HFSS) software. As shown in Figure 2(a), antenna 1 is a fold annular slot antenna, and the asymmetric of the slot width will lead to two split orthogonal degenerate modes around 2.45 GHz shown in Figure 2(b). The equivalent length of the slot is taken as one operating wavelength at the fundamental operating frequency. Similar with antenna 1, antenna 2 can be excited to yield two orthogonal degenerate modes around 5.8 GHz. Combining two different sizes of the annular slots in
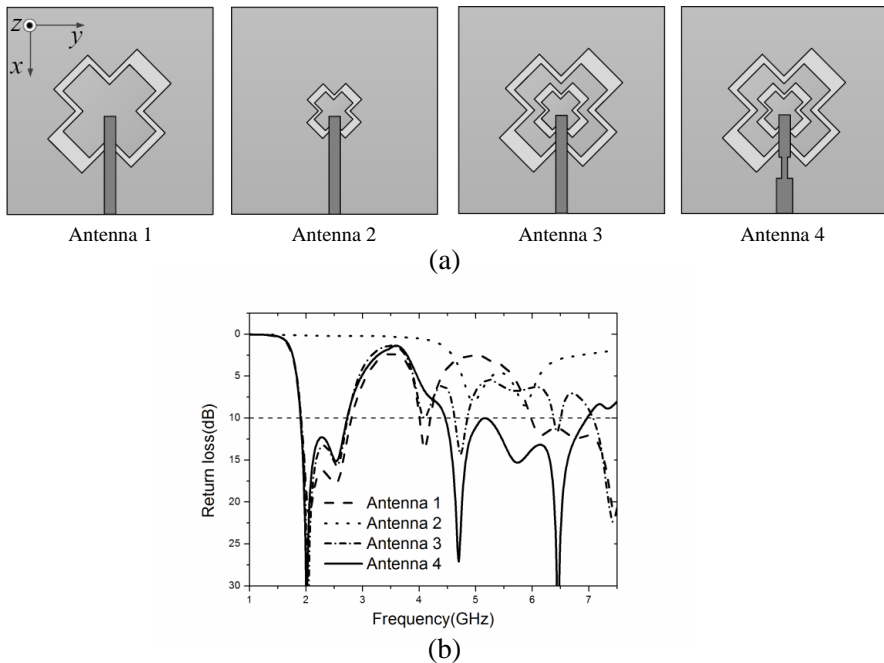

Figure 2. (a) Design evolution of the proposed antenna. (b) Corresponding simulated return losses curves.

antenna 1 and antenna 2, the double slot rings structure of antenna 3 will be obtained. Due to the fact that the proposed antenna operates in two different bands, the modified microstrip transform line is adjusted carefully so as to achieve good impedance matching in both operating bands. By building a microstrip transmission line circuit model in Advanced Design System (ADS) software, the dimensions of stepped impedance microstrip transform line are preliminarily tuned, which are further optimized via HFSS with the combination of slots on the ground plane, as shown in Table 1.

Table 1. The optimized design parameters and values.

Parameter	L_{o1}	L_{o2}	L_{i1}	L_{i2}	S_{o1}	S_{o2}	S_{i1}	S_{i2}	W_{f1}	L_{f1}
Value/mm	27	27	10.2	11.4	1.2	3.7	0.5	2	1	10
Parameter	W_{f2}	L_{f2}	W_{f3}	L_{f3}	W_1	W_2	W_3	W_4	G	h
Value/mm	0.5	5	1.4	11	11	9	4	3	50	1

3. PARAMETER ANALYSIS

The key geometrical parameters of the proposed antenna are studied in this section. The effects of these parameters on axial ratio are analyzed when only the involved parameters varied at a time.

3.1. Effects of Circumference of the Outer Slot

The effects of varying the circumference of the outer slot on the axial ratio are shown in Figure 3(a). The values of L_{o1} and L_{o2} are varied at the same time. As expected, the circumference of outer slot, determined by the L_{o1} and L_{o2}, affect the orthogonal degenerate modes at the lower frequency. The lower frequency for CP radiation decreases with the increasing of the L_{o1} and L_{o2}. It is noted that, the L_{o1} and L_{o2} can also affect the upper frequency for CP radiation, which indicates the coupling of the outer and the inner slots.

3.2. Effects of the Outer Slot Width

Figure 3(b) shows the effects of the width of the outer slot. The value of S_{o1} varies from 0.8 mm to 1.6 mm when S_{o2} maintains to be 3.7 mm. As expected, the width of outer slot has a great effect on the axial ratio of the lower frequency but little effect on the axial ratio of the upper frequency. That means the value of S_{o1} is the key parameter which determines the axial ratio of lower frequency. The value of S_{o1} should
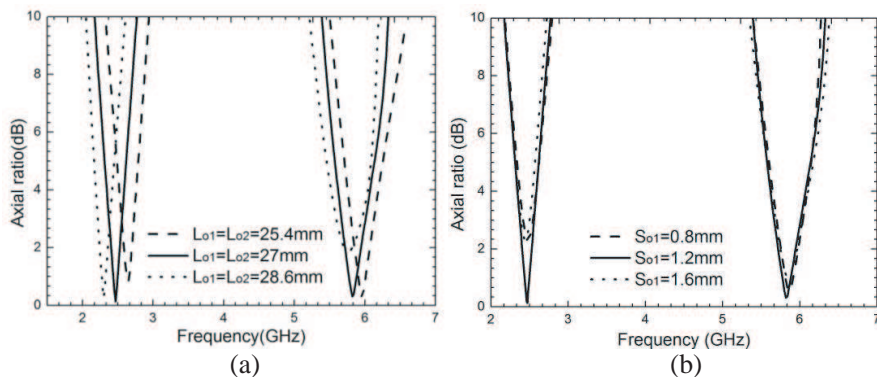
Figure 3. (a) Simulated axial ratio for different values of L_{o1} and L_{o2}. (b) Simulated axial ratio for different values of S_{o1}.

be adjusted carefully, and if it is too large ($S_{o1} = 1.6$ mm) or too small ($S_{o1} = 0.8$ mm), the CP radiation will be deteriorated obviously.

3.3. Effects of the Inner Slot Circumference

The effects of L_{i1} and L_{i2} are shown in Figure 4(a). Just like the parameters of L_{o1} and L_{o2}, L_{i1} and L_{i2} control the orthogonal degenerate modes at the upper frequency. With the circumference of the inner slot increases, the higher operation band of the antenna shifts down dramatically while the resonant frequency of the lower band changes slightly.
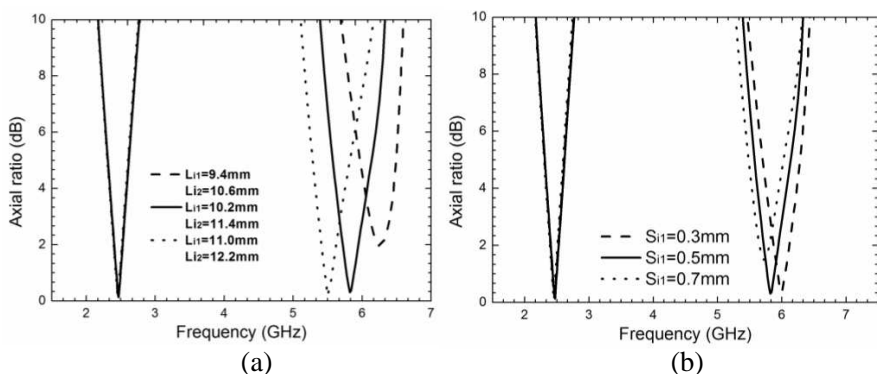

Figure 4. (a) Simulated axial ratio for different values of L_{i1} and L_{i2}. (b) Simulated axial ratio for different values of S_{i1}.

3.4. Effects of the Inner Slot Width

Figure 4(b) shows the effects of the width of the inner slot on axial ratio. The value of S_{i1} varies from 0.3 mm to 0.7 mm when S_{i2} maintains to be 2 mm. The value of S_{i1} is the key parameter controlling the axial ratio of upper frequency, and the width of the slot should be optimized to realize CP radiation at high band. If it is too large ($S_{i1} = 0.7$ mm), the CP radiation will be deteriorated. If it is too small ($S_{i1} = 0.3$ mm), the difficulty for fabrication will increase.
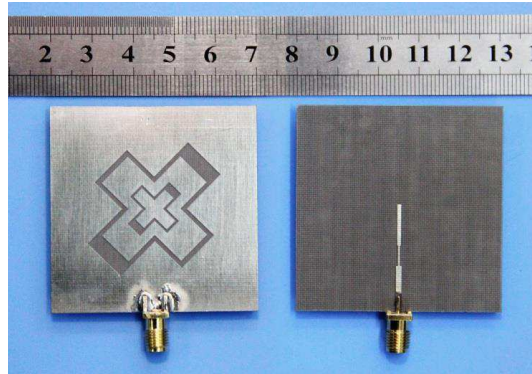

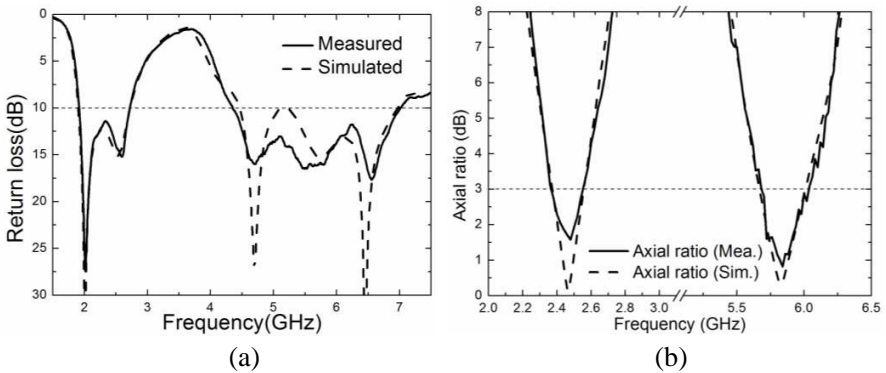**Figure 5.** Photograph of the proposed antenna.

Figure 6. The simulated and measured (a) return losses, (b) axial ratios on z-axis.
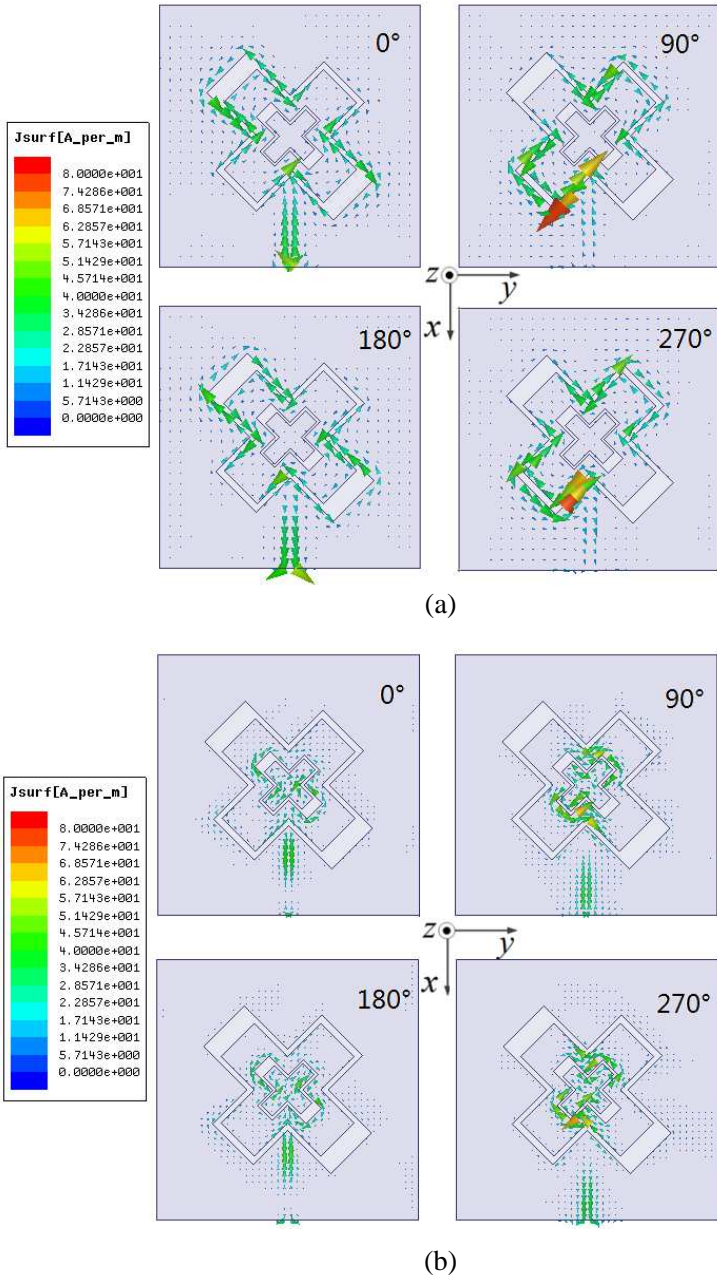
(a)

(b)

Figure 7. The simulated current distributions at the frequency of (a) 2.45 GHz (b) 5.8 GHz.

4. EXPERIMENTAL RESULTS AND DISCUSSION

A prototype of the proposed antenna is fabricated and measured. The photograph of the proposed antenna is presented in Figure 5. Experimental results are measured with the WILTRON 37269A vector network analyzer and the Near Field Antenna Measurement System, Satimo.

The simulated and measured return losses and axial-ratios on z-axis direction as shown in Figure 1 are plotted in Figure 6. As expected, the measured results show a good agreement with the simulated data. The measured impedance bandwidths (return loss $\geqslant 10\,\mathrm{dB}$) are 810 MHz (1.91–2.72 GHz) and 2640 MHz (4.36–7.00 GHz). And two
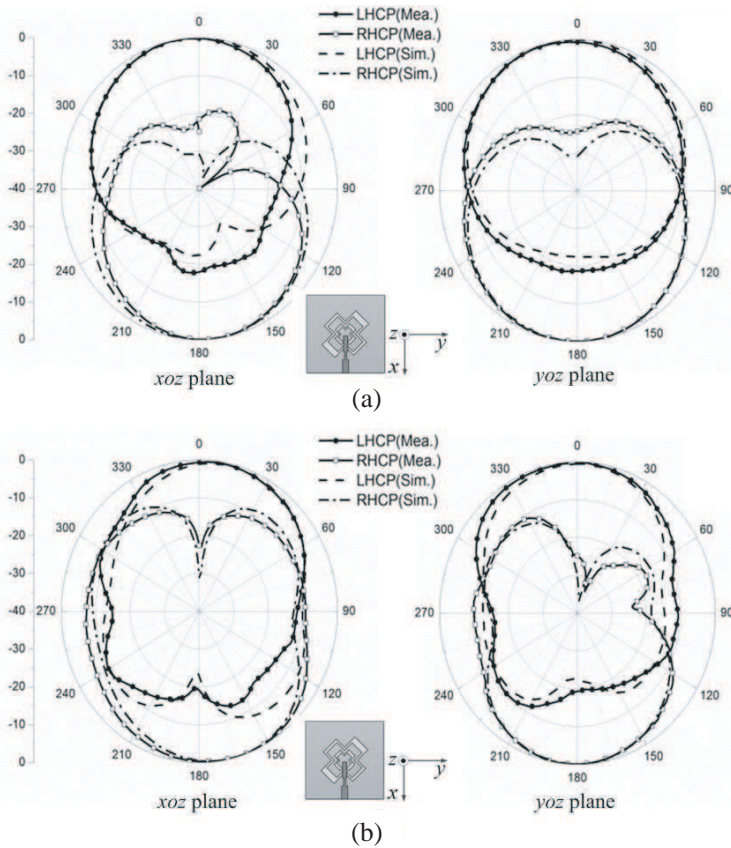

(a)

(b)

Figure 8. Simulated and measured radiation patterns at (a) 2.45 GHz, (b) 5.8 GHz.

measured 3-dB axial-ratio bandwidths (ARBW) are 200 MHz (2.36–2.56 GHz) and 360 MHz (5.68–6.04 GHz).

The simulated current distributions on the proposed antenna at the frequencies of 2.45 GHz and 5.8 GHz, presented in Figure 7, can further demonstrate the mechanism of the dual-band CP radiation. It can be observed that the current distributions are concentrated on the patch for four phase angles of 0°, 90°, 180°, and 270°, respectively. As shown in Figure 7(a), the current flows along the outer slot so that the lower resonant mode at about 2.45 GHz can be excited. Thus, the lower operation band (2.45 GHz) is mainly attributed to the outer slot. An instantaneous current phase on the proposed antenna, at 90° intervals, demonstrates a circularly polarized radiation. The current flows clockwise rotate from $+y$-axis to $+x$-axis, and result in the left-hand circularly polarized (LHCP) radiation toward the $+z$ direction. Two zeros of current distributions can be observed on the outer annular slot which indicates the slot is a full-wavelength slot. In Figure 7(b), the current flows mainly focused on the inner slot, and the 5.8 GHz resonant mode is excited. The inner slot is also a full-wavelength slot at the frequency of 5.8 GHz. The left-handed circularly polarized (LHCP) radiation toward the $+z$ direction can be explained by analyzing on the instantaneous current around the inner slot.

The simulated and measured radiation patterns at 2.45 GHz and 5.8 GHz are plotted in Figure 8. The antenna radiates a bidirectional wave with the opposite circularly polarization. The radiation of the antenna is LHCP for $z > 0$ while RHCP for $z < 0$. It can be seen that the main beam direction hardly shifts away from the zenith at the both frequencies of 2.45 GHz and 5.8 GHz.
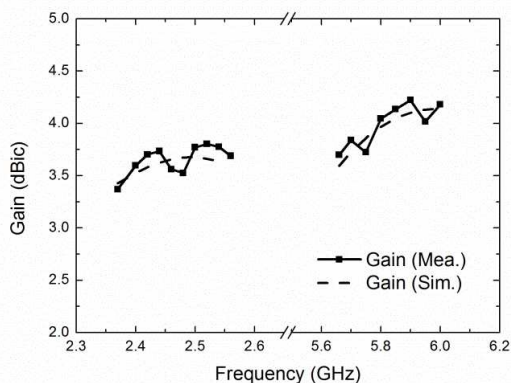

Figure 9. Simulated and measured gain.

Figure 9 shows the simulated and measured gains in the two operating bands. It can be clearly seen that the maximum gains are about 3.3–3.8 dBic at lower operating band and 3.6–4.3 dBic at the upper operating band.

5. CONCLUSION

A single-feed circularly polarized annular slot antenna for dual-broadband operation is presented in this article. By etching two fold annular slots on the ground, two desired frequencies is obtained. And circularly polarized radiation in two bands is realized by adjusting the widths of the two slots.

The experimental results show that the impedance bands cover 1.91–2.72 GHz (35.0%) at lower band and 4.36–7.00 GHz (46.5%) at higher band, as well as the 3-dB axial ratio bandwidths are 2.36–2.56 GHz (8.1%) and 5.68–6.04 GHz (6.1%), respectively. The peak gains are about 3.3–4.3 dBic at the operating bands. As a result, the antenna can be applied to 2.45/5.8 GHz RFID or 2.4/5.8 GHz WLAN communication systems.

REFERENCES

1. Chen, J.-S., "Dual-frequency annular-ring slot antennas fed by CPW feed and microstrip line feed," *IEEE Trans. on Antennas and Propag.*, Vol. 53, No. 1, 569–571, Jan. 2005.

2. Sze, J.-Y., T.-H. Hu, and T.-J. Chen, "Compact dual-band annular-ring slot antenna with meandered grounded strip," *Progress In Electromagnetics Research*, Vol. 95, 299–308, 2009.

3. Lee, Y.-C. and J.-S. Sun, "Compact printed slot antennas for wireless dual- and multi-band operations," *Progress In Electromagnetics Research*, Vol. 88, 289–305, 2008.

4. Eldek, A.-A., A.-Z. Elsherbeni, and C.-E. Smith, "Dual-wideband square slot antenna with a u-shaped printed tuning stub for personal wireless communication systems," *Progress In Electromagnetics Research*, Vol. 53, 319–333, 2005.

5. Tiang, J.-J., M.-T. Islam, N. Misran, and J.-S. Mandeep, "Circular microstrip slot antenna for dual-frequency RFID application," *Progress In Electromagnetics Research*, Vol. 120, 499–512, 2011.

6. Yang, S.-S., K.-F. Lee, A.-A. Kishk, and K.-M. Luk, "Design and study of wideband single feed circularly polarized microstrip

antennas," *Progress In Electromagnetics Research*, Vol. 80, 45–61, 2008.

7. Deng, J.-Y., L.-X. Guo, T.-Q. Fan, Z.-S. Wu, Y.-J. Hu, and J.-H. Yang, "Wideband circularly polarized suspended patch antenna with indented edge and gap-coupled feed," *Progress In Electromagnetics Research*, Vol. 135, 151–159, 2013.

8. Sun, L., Y.-H. Huang, J.-Y. Li, and Q.-Z. Liu, "A wideband circularly polarized candy-like patch antenna," *Journal of Electromagnetic Waves and Applications*, Vol. 25, Nos. 8–9, 1113–1121, 2011.

9. Sze, J.-Y. and S.-P. Pan, "Design of broadband circularly polarized square slot antenna with a compact size," *Progress In Electromagnetics Research*, Vol. 120, 513–533, 2011.

10. Lin, Y.-F., Y.-K. Wang, H.-M. Chen, and Z.-Z. Yang, "Circularly polarized crossed dipole antenna with phase delay lines for RFID handheld reader," *IEEE Trans. on Antennas and Propag.*, Vol. 60, No. 3, 1221–1227, Mar. 2012.

11. Nayeri, P. and K.-F. Lee, "Dual-band circularly polarized antennas using stacked patches with asymmetric U-slots," *IEEE Antennas and Wireless Propagation Letters*, Vol. 10, 492–495, 2011.

12. Hsieh, W.-T., T.-H. Chang, and J.-F. Kiang, "Dual-band circularly polarized cavity-backed annular slot antenna for GPS receiver," *IEEE Trans. on Antennas and Propagat.*, Vol. 60, No. 4, 2076–2080, Apr. 2012.

13. Bao, X.-L. and M.-J. Ammann, "Monofilar spiral slot antenna for dual-frequency dual-sense circular polarization," *IEEE Trans. on Antennas Propagat.*, Vol. 59, No. 8, 3061–3065, Aug. 2011.

14. Chen, Q., H.-L. Zheng, J.-H. Hu, and S.-G. Jiang, "Design of CPW-fed dual-band circularly-polarized annular slot antenna with two perturbation strips," *Progress In Electromagnetics Research C*, Vol. 28, 195–207, 2012.

15. Heidari, A.-A., M. Heyrani, and M. Nakhkash, "A dual-band circularly polarized stub loaded microstrip patch antenna for GPS applications," *Progress In Electromagnetics Research*, Vol. 92, 195–208, 2009.